View metadata, citation and similar papers at core.ac.uk
brought to you by CORE
provided by Xiamen University Institutional Repository

Cite this: *Phys. Chem. Chem. Phys.*, 2011, **13**, 16741–16747

www.rsc.org/pccp

PAPER

Studies on the interaction of achiral cationic pseudoisocyanine with chiral metal complexes

Jian Wang,*[a] Lixi Zeng,[a] Dongdong Ding,[b] Xiangjun Li,[a] Hui Zhang,*[b] Hong Zhao,*[a] Jun Fan,[d] Weiguang Zhang*[d] and Yujian He*[ac]

Received 22nd February 2011, Accepted 28th July 2011
DOI: 10.1039/c1cp20470j

Published on 22 August 2011 on http://pubs.rsc.org | doi:10.1039/C1CP20470J
Downloaded by Xiamen University on 07 April 2012

The effect of chiral metal complexes ($[Co(en)_3]I_3{\cdot}H_2O$, *cis*-$[CoBr(NH_3)(en)_2]Br_2$, $K[Co(edta)]{\cdot}2H_2O$ and $[Ru(phen)_3](PF_6)_2$) on the polymer-bound J-aggregates in aqueous mixtures of pesudoisocyanine (PIC) iodine and poly(acrylic acid, sodium)(PAAS) have been studied by UV–vis absorption, circular dichroism (CD) and fluorescence spectra. At low concentration, the PIC monomers could self-assemble to form supermolecules by binding to each of the COO^- groups on the polymer chains through electrostatic interactions. After the addition of chiral metal complexes to the formed PIC-PAAS J-aggregates, we found that only the chiral multiple π-conjugated phenanthroline metal complexes could transfer their metal-centered chiral information to the formed J-aggregates. The chiral J-aggregates showed a characteristic induced circular dichroism (ICD) in the visible region of J-band chromophore, and the ICD signals depend on the absolute configuration, concentration of the chiral multiple π-conjugated metal complexes, as well as temperature. More interestingly, the supramolecular chirality of the polymer supported PIC J-aggregates could be memorized even after the addition of an excess opposite chiral complex enantiomers. This is in sharp contrast to the behavior in the high concentrated NaCl induced PIC-J aggregates, in which the optical rotation of a mixture of two enantiomers varies linearly with their ratio.

1. Introductions

The challenge of generating chirality at different hierarchical levels is particularly evident in the context of supramolecular self-assembly.[1–3] Unlike molecular chirality, the highly complex supramolecular structures are generated through molecular recognition-driven self-assembly. This kind of asymmetry is dominated by "weak", non-covalent bonds. Driving forces such as π–π stacking,[4–11] hydrogen bonds,[12–21] electrostatic interaction,[22–24] coordination,[25–31] and hydrophobic interaction[32–35] are often utilized to organize molecules to create ordered structures with specific functionality.

The water-soluble cationic cyanine dye molecule (1,1′-diethyl-2,2′-cyanine, PIC, Scheme 1) is an excellent building block for assembling supramolecular architectures.[36–38] One of the most studied phenomena related to this dye is the formation of supramolecular assemblies called J-aggregates which was observed by Jelley[39] and Scheibe[40] nearly 70 years ago. The specific structures of the J-aggregates are typical of a head-to-tail intermolecular association between the molecular units.[41–43] Preference for the PIC cations to form J-aggregates

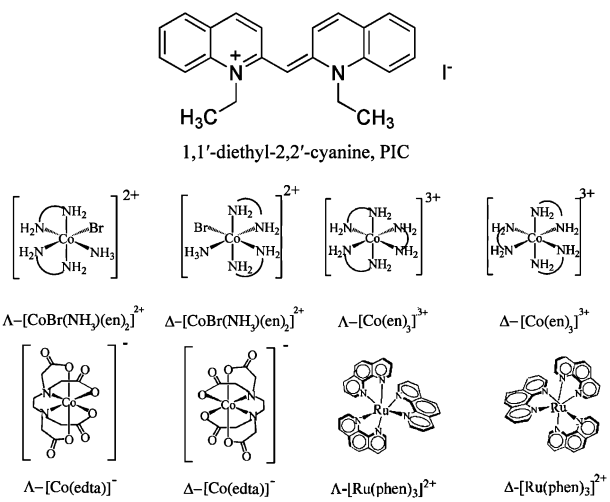

Scheme 1 Chemical structures of PIC and the chiral metal complexes.

[a] *College of Chemistry and Chemical Engineering, Graduate University of Chinese Academy of Sciences, Beijing 100049, China. E-mail: wangjian06@mails.gucas.ac.cn, heyujian@gucas.ac.cn, hongzhao@gucas.ac.cn; Fax: (+86) 10-8825-6093; Tel: (+86) 10-8825-6141*
[b] *College of Chemistry and Chemical Engineering, Xiamen University, Xiamen 361005, China. E-mail: huizhang@xmu.edu.cn; Tel: (+86) 592-2183910*
[c] *State Key Laboratory of Natural and Biomimetic Drugs, Peking University, Beijing, China*
[d] *School of Chemistry and Environment, South China Normal University, Guangzhou, 510006, China*

Published on 22 August 2011 on http://pubs.rsc.org | doi:10.1039/C1CP20470J
Downloaded by Xiamen University on 07 April 2012

rather than the generally more common H-aggregates is mainly due to the molecular structure of PIC. The cations bear two hydrophobic ethyl groups, which are close to the center of the molecule, thus preventing the formation of sandwich-type assemblies called H-aggregates. For their unique planar as well as rigid molecular geometry, well-ordered assemblies of these functional materials are found potential applications in supramolecular devices, smart materials, and machines.[44–47] The inherent self-assembling properties of cyanine molecules with specific directional non-covalent links are projected for the construction of molecular receptors with well-defined geometry.

Increasing interests in the chirality of cyanine supermolecules are relevant not only to understand the chiral bias inherent in life but also to their potential applications.[48,49] The induced optical activity of cyanine dye J-aggregates have been achieved by the induction of large biopolymers such as proteins,[50,51] oligopeptides,[52] polysaccharids,[53] DNA,[54] and small molecules such as amino acids.[55] However, one basic question is still open: exactly how the weak non-covalent interaction among the local chirality of a small molecule translates to global helicity of preferred handedness in supermolecules still remains to be elucidated.

In our previously reported work, we found the random symmetry breaking in the synthesis of chiral octahedral cobalt complex (*cis*-[CoBr(NH_3)(en)$_2$]Br_2) could be transferred in the supramolecular self-assembly process of anion porphyrin derivates.[56] In order to understand the mechanism of the chiral induction process, chiral metal complexes with different structures (Scheme 1) were added to the acid porphyrin solution. It was found that only the chiral cationic complexes could cause the self-assembly process of the anion porphyrin derivates, accompany with their chiral information transferred to the formed J-aggregates. It indicated the driving force of the chirality transformation process is dominated by the electrostatic force between the cationic chiral complexes and anionic porphyrin derivates.[57]

In this work, we further investigated the effect of chiral metal complexes on the self-assembly process of the cationic PIC molecules. The results show in anionic polyelectrolyte (PAAS) solution, that the PIC monomer could self-assemble to form J-aggregates. It was interesting to find that only the addition of chiral [Ru(phen)$_3$](PF_6)$_2$, which has a multiple π-conjugated system in the structure could transmit its chiral information into the formed J-aggregates. The induced CD signal depends on the absolute configuration, the concentration of the chiral metal complex and the temperature. The supramolecular in the PIC J-aggregates can be memorized even after the addition of an excess of phenanthroline with an opposite chirality. These findings provide an insight into the generation of supramolecular chirality by the non-covalent interactions.

2. Experimental

2.1 Materials

1,1′-diethyl-2,2′-cyanine (pseudoisocyanine, PIC, Aldrich), Poly(arylic acid, sodium salt), 35 wt% solution in water (PAAS, Aldrich) were used as received without further purification.

The chiral metal complexes used in this work are synthesized according to the reported literatures.[58–62]

2.2 Chiral assembly of the PIC induced by polyelectrolyte

A solution of PIC (3×10^{-4} mol L^{-1}) was freshly prepared by dissolving the 1,1′-diethyl-2,2′-cyanine crystal in Milli-Q water. The stock solutions of Λ-/Δ-*cis*-[CoBr(NH_3)(en)$_2$]Br_2, Λ-/Δ-[Co(en)$_3$]I_3·H_2O, Λ-/Δ-K[Co(edta)]·2H_2O, and Λ-/Δ-[Ru(phen)$_3$](PF_6)$_2$ (3 mM), were prepared by dissolving them in water. The PIC J-aggregates was formed by adding PAAS (1 g L^{-1}, 5 μL) into PIC solution (3×10^{-5} mol L^{-1}, 1 mL). In order to investigate the chiral effect on the polymer-bound PIC J-aggregates, chiral metal complexes with different structures at the same concentration were added to the system. The samples were kept in dark at room temperature before characterizing.

2.3 Temperature-dependent experiment on the chiral self-assembly process

The temperature dependent experiment was conducted by placing the chiral J-aggregate solution in a cell, and heated to 80 °C in water bath. The UV-vis and CD spectra was recorded during its cooling process.

2.4 Chiral memorezation in the suparmolecular J-aggregates

The stock solutions of chiral J-aggregates induced by Λ-[Ru(phen)$_3$](PF_6)$_2$ ([PIC] = 3×10^{-5} mol L^{-1}, [PAAS] = 5 mg L^{-1}, [Λ-[Ru(phen)$_3$](PF_6)$_2$] = 0.05 mM, 2 μL) were incubated at room temperature and were characterized by UV and CD spectroscopy. Then, the opposite configurational Δ-[Ru(phen)$_3$](PF_6)$_2$ complex with different concentrations were added to these sample (1 μL to 6 μL, 0.05 mM). After stabilized, these samples were characterized by UV and CD spectroscopy again to investigate the "chiral memory" effect.

2.5 Characterizing

The adsorption and CD spectra were measured using a UV-2550 spectrophotometer (Japan) and a Jasco J-810 spectropolarimeter (Japan), respectively. Fluorescence spectra were obtained on an LS 55 fluorescence spectrometer (Perkin–Elmer). The size of the quartz cell is 0.5 cm. Atomic force microscopy (AFM) images were recorded on a Veeco Dimesion 3100 atomic force microscope (Digital Instruments, USA) with a tapping mode.

3. Results and disscussions

3.1 Formation of PIC J-aggregates triggered by anionic polyelectrolyte

It is well known that the PIC dye molecules could form J-aggregates at high concentrations ($>10^{-3}$ M) in a concentrated salt solution ($\approx$5 M).[63,64] One-dimensional J-aggregates of well-defined size can be also formed by binding dye molecules to polyelectrolytes, such as poly(vinyl sulfonic acid sodium salt). The driving force for the formation of dye-polymer assemblies is through the electrostatic interaction of cationic dyes with the negatively charged groups on the polymer chain. In this article, we used poly(arylic acid, sodium salt) (PAAS) as a negative support to form PIC assemblies.

 This journal is © the Owner Societies 2011

Published on 22 August 2011 on http://pubs.rsc.org | doi:10.1039/C1CP20470J
Downloaded by Xiamen University on 07 April 2012

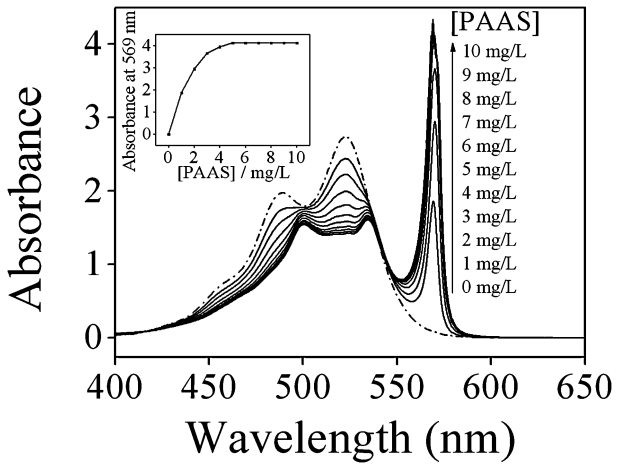

Fig. 1 UV-vis absorption spectra changes of the PIC solution (3×10^{-5} mol L^{-1}) with different PAAS concentration at room temperature. The dashed line indicates the absorption spectrum of PIC solution without PAAS. The insets shows the absorption intensity at 568 nm changes towards the concentration of PAAS.

Fig. 1 shows the effect of PAAS concentration on the formation of PIC J-aggregates in 3×10^{-5} mol L^{-1} diluted PIC aqueous solution. UV–vis absorption spectra of the diluted PIC solution without PAAS had only one maximum at 520 nm and a short wavelength shoulder at 490 nm (dashed dot line). This spectrum does not indicate any significant amount of dimmers or other aggregates present in the solution. Therefore, we can conclude that at a concentration of 3×10^{-5} mol L^{-1}, PIC exists mostly in a monomeric form in pure water.

However, the addition of PAAS at 1 mg L^{-1} to the PIC solution caused a significant change in the UV–vis spectra. An intense narrow absorption band appeared at 569 nm, and the absorption band at 490 nm and 520 nm became degenerated. The further addition of PAAS to 2 mg L^{-1} caused the appearance of two additional less intense broad absorption peaks at 499 nm and 534 nm. With the increasing of PAAS concentration, the absorption peak at 490 nm and 520 nm decreased, together with the absorption intensity at 568 nm increased. While the concentration of PAAS is up to 5 mg L^{-1}, the absorbance at 490 nm and 520 nm was totally disappeared and red-shifted to 499 nm and 534 nm, respectively. In addition, the absorption at 568 nm reaches a maximum. Then, the 5 mg L^{-1} of the optimal PAAS concentration in the following experiments was selected.

3.2 The effect of chiral metal complexes on the formed PIC J-aggregates

In order to investigate the effect of metal complexes on the PIC J-aggregate formed in PAAS solution, different metal complexes with the same concentration (0.1 μM) were added to the solution after the J-aggregates were formed. In Fig. 2, the UV–vis absorption results show that after the addition of $[Co(en)_3]I_3{\cdot}H_2O$(Fig. 2A), the absorption at 568 nm vanished and the absorption at 490 nm and 520 nm recovered(dashed line), indicating the PIC J-aggregates dissociated into monomer. And, the addition of *cis*-$[CoBr(NH_3)(en)_2]Br_2$ (Fig. 2B) and

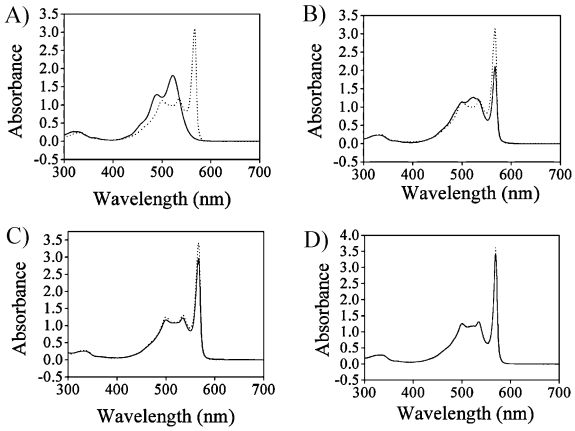

Fig. 2 UV–vis absorption spectral changes of the PIC-PAAS J-aggregates after the addition of 0.1 μM of $[Co(en)_3]I_3{\cdot}H_2O$, *cis*-$[CoBr(NH_3)(en)_2]Br_2$, $K[Co(edta)]{\cdot}2H_2O$ and $[Ru(phen)_3](PF_6)_2$ (dot line), the solid line is the PIC-PAAS J-aggregates without any metal complexes. ([PIC] = 3×10^{-5} M, [PAAS] = 5 mg/L).

$K[Co(edta)]{\cdot}2H_2O$ (Fig. 2C) shows only an absorption decrease at 568 nm. However, the addition of $[Ru(phen)_3](PF_6)_2$ (Fig. 2D) at 0.1 μM have no significant effect on the absorption spectra of the J-aggregates.

To better understand the effect of the above metal complexes on the formed polymer-bound PIC J-aggregates, the titration experiment of the metal complexes were conducted. The results were shown in Fig. 3. Fig. 3A shows the absorption intensity of the J-band decreased by 10%, 32%, 77% and 97% after $[Co(en)_3]I_3{\cdot}H_2O$ was added at 0.02 μM, 0.04 μM, 0.06 μM and 0.08 μM, respectively. When the concentration of the metal complex was 0.1 μM, the absorption of the J-band at 568 was disappeared totally. Fig. 3B shows the effect of *cis*-$[CoBr(NH_3)(en)_2]Br_2$ on the formed polymer-bound PIC J-aggregates. It shows that after the addition of this metal complex at the concentration of 0.02 μM to 0.1 μM caused the

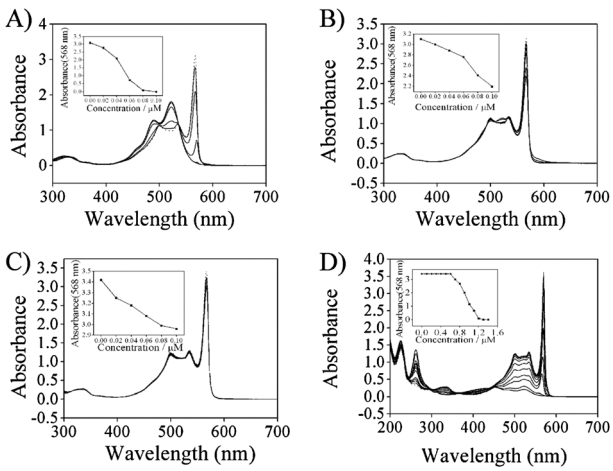

Fig. 3 UV–vis absorption spectral changes of the PIC-PAAS J-aggregates towards the concentration of different metal complexes. (A) $[Co(en)_3]I_3{\cdot}H_2O$; (B) *cis*-$[CoBr(NH_3)(en)_2]Br_2$; (C) $K[Co(edta)]{\cdot}2H_2O$; (D) $[Ru(phen)_3](PF_6)_2$. All the dot line in the Figures are the PIC-PAAS J-aggregates without the addition of metal complexes. ([PIC] = 3×10^{-5} M, [PAAS] = 5 mg L^{-1}).

Published on 22 August 2011 on http://pubs.rsc.org | doi:10.1039/C1CP20470J
Downloaded by Xiamen University on 07 April 2012

$$PIC^+ I^- + PAAS \rightleftharpoons PIC\text{-}PAAS\ (J\text{-}aggregates) + I^-$$

Scheme 2 Schematic illustration of the electrostatic forece induced self-assembly of PIC^+I^- molecules.

absorption intensity of J-band decreased by 3%, 7%, 11%, 22% and 29%, respectively. Fig. 3C also shows that the addition of K[Co(edta)]·$2H_2O$ to the formed J-aggregates could cause an absorption intensity decrease of the J-band at 568 nm. However, the spectra change after the addition $[Ru(phen)_3](PF_6)_2$ in Fig. 3D shows a little bit different to the above results. We can see that at a low concentration of chiral $[Ru(phen)_3](PF_6)_2$ (0.1 μM–0.6 μM), the characteristic absorbance of the PAAS-PIC J-aggregates at 568 nm does not change too much compared to the sample which no chiral $[Ru(phen)_3](PF_6)_2$ was added. This clearly indicated that $[Ru(phen)_3](PF_6)_2$ have little effect on the amounts of the PIC-PAAS J aggregates. However, the further addition of $[Ru(phen)_3](PF_6)_2$ caused the decrease of the absorption at 499 nm, 534 nm and 569 nm. When the concentration of $[Ru(phen)_3](PF_6)_2$ is up to 1.4 μM, the absorption of the PIC molecules were almost totally bleached.

The absorption spectral change of the PIC-PAAS J-aggregates after the addition of the metal complex is due to the shift of the balance (Scheme 2). According to the reported literature, the polymer-bound PIC J-aggregates are extremely sensitive to the ionic strength of the solution.[65] The addition of inorganic salts to the system increased the ionic strength, and caused the shift of the equilibrium. When $[Co(en)_3]I_3·H_2O$ was added, the import of I^- in the solution caused the shift of the balance, which makes the dissociation of the PAAS-PIC J-aggregates into monomer.

It is well known the monomeric PIC dye (λ_{max} = 523 nm, ε = 77 000 L mol^{-1} cm^{-1}) does not exhibit fluorescence, due to fast thermal deactivation by the flip–flop motion of the two chinolyl ring systems, which are twisted to each other.[66,67] However, when the PIC-PAAS J-aggregates formed, it could exhibit a strong fluorescence. Then, fluorescence emission spectral experiments for the solutions of 3×10^{-5} mol L^{-1} PIC-PAAS J-aggregates with different chiral complexes were obtained (Fig. 4). Without any metal complexes, the fluorescence spectrum consists of an intense resonance fluorescence band at 575 nm with a small secondary peak at 613 nm (solid line). We could find the addition of $[Co(en)_3]I_3·H_2O$ (dashed dot line) caused the fluorescent quenching. And, the addition of K[Co(edta)]·$2H_2O$(dot line) and *cis*-$[CoBr(NH_3)(en)_2]Br_2$ (not shown) caused a decrease of the fluorescent. However, $[Ru(phen)_3](PF_6)_2$ (dashed line) have no significant obvious effect on the fluorescence spectra of the PIC-PAAS J-aggregates. These results can further indicate the PIC-PAAS aggregate is very sensitive to the ionic strength and its counter ion.

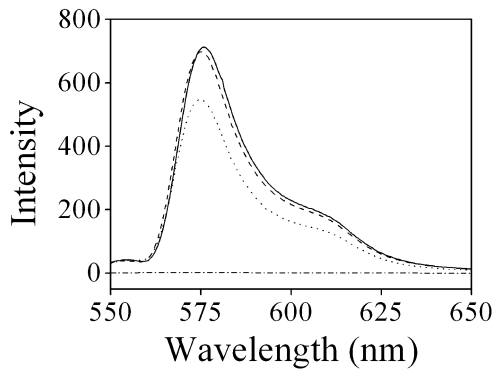

Fig. 4 Fluorescence spectrum changes of the PIC-PAAS J-aggregates (solid line) and after the addition of 0.1 μM of $[Co(en)_3]I_3·H_2O$ (dashed dot line), K[Co(edta)]·$2H_2O$ (dot line), and $[Ru(phen)_3](PF_6)_2$ (dashed line). [PIC] = 3×10^{-5} M, [PAAS] = 5 mg L^{-1}.

3.3 Circular dichroism of PIC J-aggregates induced with different chiral-only-at-metal complexes

The interaction between the chiral metal with the PIC J-aggregates was further investigated by CD spectra. The results were shown in Fig. 5. A strong bisignated Cotton effect in the J-band chromophore region was appeared after chiral $[Ru(phen)_3](PF_6)_2$ was added to the system, and the signals of the ICDs were mirror-image which were dependent on the absolute configuration of the chiral $[Ru(phen)_3](PF_6)_2$ complexes. The chiral PIC J-aggregates with Λ-$[Ru(phen)_3](PF_6)_2$ showed two positive CD signals at 560 nm and 486 nm, and two negative CD signals at 532 nm and 499 nm, respectively (solid line). While its enantiomer Δ-$[Ru(phen)_3](PF_6)_2$ is used, the CD spectrums of the formed J-aggregates are nearly mirror-imaged with two crossovers at 547 nm and 492 nm (dashed line). The Cotton effect at 269 nm and 257 nm belongs to chiral $[Ru(phen)_3](PF_6)_2$.

However, the additions of chiral K[Co(edta)]·$2H_2O$, *cis*-$[CoBr(NH_3)(en)_2]Br_2$ and $[Co(en)_3]I_3·H_2O$ to the PAAS-PIC J-aggregates do not cause any obvious Cotton effect in their CD spectra(data not shown). This indicated that these chiral metal complexes could not guide the handedness of the aggregates. Compared to these chiral metal complexes, we can obviously see that only the chiral center of $[Ru(phen)_3](PF_6)_2$ is multiple π-conjugated. Different to the anionic porphyrin system, in which the chiral assembly process was governed by the electrostatic force. The handeness of the polymer-bound PIC J-aggregates were dominated by the π–π stacking between the aromatic rings.

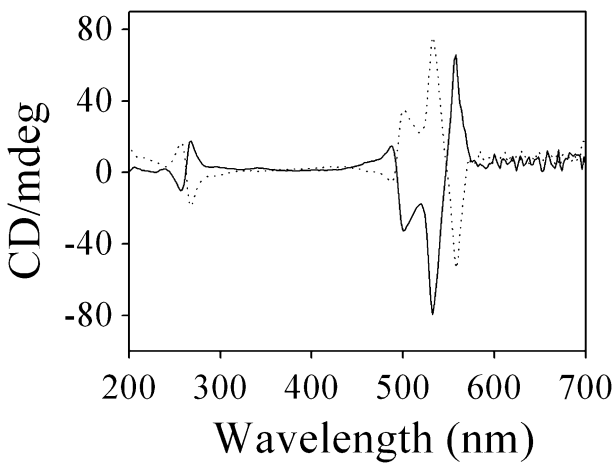

Fig. 5 CD spectra of the induced PIC-PAAS J-aggregates with Λ-, or Δ-$[Ru(phen)_3](PF_6)_2$. [PIC] = 3×10^{-5} M, [PAAS] = 5 mg L^{-1}, [Λ-$[Ru(phen)_3](PF_6)_2$] = 0.1 μM, [Δ-$[Ru(phen)_3](PF_6)_2$] = 0.1 μM.

 This journal is © the Owner Societies 2011

Published on 22 August 2011 on http://pubs.rsc.org | doi:10.1039/C1CP20470J
Downloaded by Xiamen University on 07 April 2012

3.4 Effect of Λ-/Δ-[Ru(phen)$_3$](PF$_6$)$_2$ concentration on chiral induction of PIC-J aggregates

The concentration effect of Λ-, or Δ-[Ru(phen)$_3$](PF$_6$)$_2$ on chiral induction in PIC J-aggregates was further investigated. Fig. 6 shows the CD spectra change of 3×10^{-5} mol/L PIC in PAAS solution with the increase of Λ-, and Δ-[Ru(phen)$_3$](PF$_6$)$_2$ concentration from (0.1 μM−0.6 μM). As expected, we found the CD intensity have a concentration-dependent effect. With the increase of the concentration of the chiral metal complexes, the ICD intensity of the polymer-bound PIC J-aggregates increased simultaneously. According to the UV–vis spectra change, the addition of [Ru(phen)$_3$](PF$_6$)$_2$ at the concentration of 0.1 μM to 0.6 μM do not cause any difference in the J-band, we could speculate that the supramolecular chirality of the PIC J-aggregates is sterically affected by the aymmetric environment generated by the chiral metal complexes though non-covalent interaction. When the concentration of chiral [Ru(phen)$_3$](PF$_6$)$_2$ is up to 0.7 μM, it caused the degradation of PIC molecules, so the ICD signal also became degraded. The formation of chiral PIC-PAAS J-aggregates is due to the electrostatics force beweent the anionic polyelectrolyte and cationic PIC molecules and the π–π stacking effect of the multiple π-conjugated chiral [Ru(phen)$_3$](PF$_6$)$_2$ with PIC monomers. The chiral metal complex affected the configuration of the J-aggregates rather than its amount. With increasing Λ-, or Δ-[Ru(phen)$_3$](PF$_6$)$_2$ concentration, the conformation of the PIC J-aggregate could change from a relaxed helix to a tight state.

3.5 Temperature-dependent in the chiral self-assembly process

In order to investigate the thermodynamic stability of the chiral self-assembly process, the effect of temperature on the formed J-aggregates was further investigated. The UV-vis spectrum of the PIC-J aggregates towards the temperature was shown in Fig. 7A. The absorbance at 568 nm gradually decreased with the increasing of temperature. When the temperature is up to 80 °C, the absorption at 534 nm shifted to 522 nm, indicating the increasing of temperature caused the dissociation of the J-aggregates. However, due to their strong interaction between the cationic PIC molecules and anionic polyelectrolyte (PAAS), the PIC J-aggregates could not be totally dissociated. While cooling the solutions to room temperature, the PIC J-aggregates could be regenerated again.

The CD spectra change towards the temperature was shown in Fig. 7B. After heated, the ICD signal of the samples gradually decreased. That is because the chiral J-aggregates dissociated into monomers with the intrinsically achiral structure at a relatively high temperature. During its cooling process, the ICD signal of the PIC J-aggregates increased gradually until reaching its maximum at room temperature. This is consistent with the UV–vis absorption results. It was worth to note that the UV–vis absorption and the ICD signals of the PIC J-aggregates showed no obviously change upon heating and cooling in several cycles.

3.6 Chirality memorization in the PIC-PAAS J-aggreagates

In order to investigate the dynamic behaviors of the chiral PIC J-aggregates, the majority-rules was performed for the enantiomers Λ-[Ru(phen)$_3$](PF$_6$)$_2$ and Δ-[Ru(phen)$_3$](PF$_6$)$_2$ in this system.

Fig. 8A shows the change in the CD spectra upon consecutive additions of different volumes of 1–6 μL of a 0.05 mM solution of Δ-[Ru(phen)$_3$](PF$_6$)$_2$ to 2 μL of a 0.05 mM solution of Λ-[Ru(phen)$_3$](PF$_6$)$_2$ induced PAAS-PIC chiral J-aggregates. At the wavelength of 257 nm and 269 nm, we can see the shape of the CD effect does not depend on the ratio of the two enantiomers. However, their intensity does depend on the ee value. That is, the initial positive CD effect weakens its intensity when the ee is reduced. Adding more Δ-[Ru(phen)$_3$](PF$_6$)$_2$ results in the appearance of a negative CD effect.

Different to our reported literature,[55] the supramolecular chiral signal of the PIC J-aggregates which were formed in a high concentrated NaCl solution could be inversed when the excess chiral inducer with the opposite configuration was added.[55] In this work, the ICD signals of the PAAS-PIC J-aggregates at 560 nm, 532 nm and 499 nm of the optically active PIC J-aggregates that was formed in the anionic polyelectrolyte do not reversed. Moreover, the CD intensity does not show too much change. This mechanism of the chiral memory phenomena is due to the strong electrostatic interaction between the cationic PIC molecules and the anionic polyelectrolyte PAAS. Since PAAS is flexible and possesses many negatively charged groups to bind the positively charged

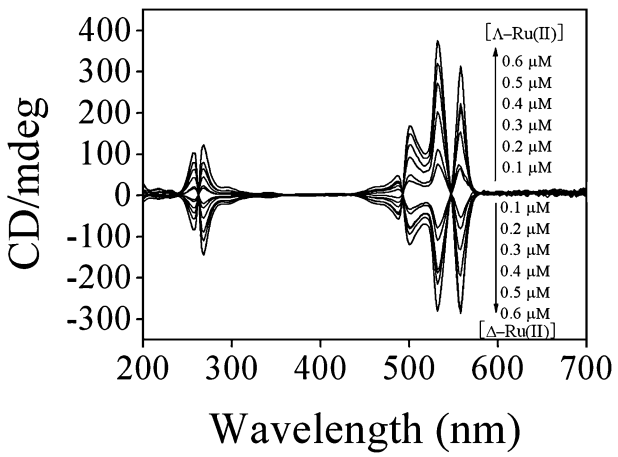

Fig. 6 Mirror-image CD spectral changes of the PIC-PAAS J-aggregates with different concentrations of chiral [Ru(phen)$_3$](PF$_6$)$_2$ complexes, [PIC] = 3×10^{-5} M, [PAAS] = 5 mg/L.

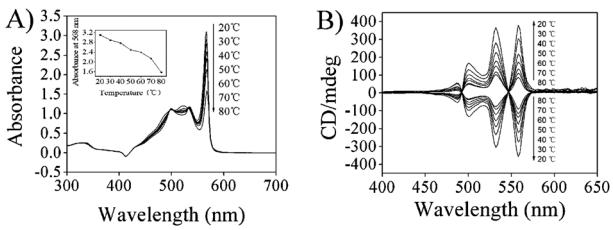

Fig. 7 (A) UV-vis absorption spectra changes of the PIC-PAAS J-aggregates at different temperatures. Inset shows PIC-PAAS J-aggregates absorbance at 568 nm with different temperatures; (B) Temperature-dependent CD spectral changes of the chiral PIC-PAAS J-aggregates, [PIC] = 3×10^{-5} M, [PAAS] = 5 mg/L, [Λ-[Ru(phen)$_3$](PF$_6$)$_2$] = 0.6 μM, [Δ-[Ru(phen)$_3$](PF$_6$)$_2$] = 0.6 μM.

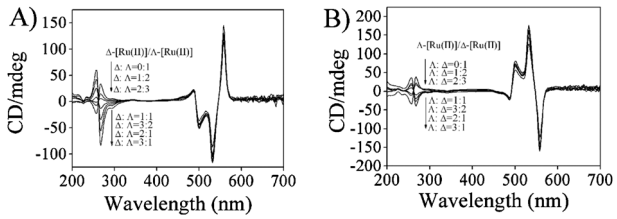

Fig. 8 (A) CD spectral changes of the chiral PIC-PAAS J-aggregates with different ratios of Λ-$[Ru(phen)_3](PF_6)_2$ to Δ-$[Ru(phen)_3](PF_6)_2$; (B): (A): CD spectral changes of the chiral PIC-PAAS J-aggregates with different ratios of Δ-$[Ru(phen)_3](PF_6)_2$ to Λ-$[Ru(phen)_3](PF_6)_2$.

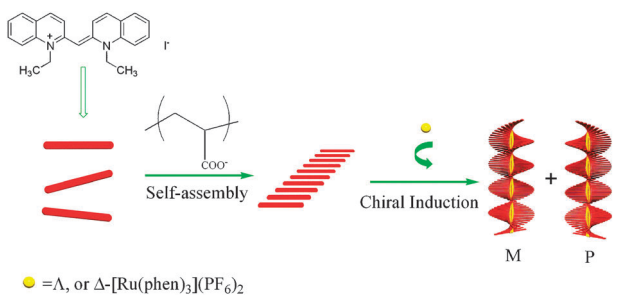

Scheme 3 Schematic illustration of the formation of chiral PIC-PAAS J-aggregates induced by the multiple π-conjugated chiral metal complex.

PIC molecules. Once the multiple π-conjugated chiral phenanthroline added to the system, it twisted the configuration of the J-aggregates. However, the followed addition of the opposite chiral phenanthroline could not further change the helical direction of the previously formed chiral PIC J-aggregates.

Similarly, if Δ-$[Ru(phen)_3](PF_6)_2$ was firstly used, after stabilized, the addition of Λ-$[Ru(phen)_3](PF_6)_2$ to the previously formed chiral PIC J-aggregates have a similar results, as shown in Fig. 8B.

3.7 Possible mechanism of the interaction of PIC with chiral $[Ru(phen)_3](PF_6)_2$

Based on the above experimental results, a possible mechanism for the chirality induction of PIC-J aggregates is proposed, as shown in Scheme 3. Firstly, the anionic polyelectrolyte could cause the aggregation of cationic PIC molecules by the electrostatic interaction to form an edge-to edge achiral J-aggregates. The driven force of the supramolecular chirality induction is based on the chiral multiple π-conjugated phenanthroline interact with the PIC J-aggregates though π–π stacking interaction. That is, the addition of multiple π-conjugated chiral phenanthroline twisted the configuration of the J-aggregates and leads to the formation of either right- or left-handed screw structures. The chiral center of the metal complex could guide the helical direction of the formed PIC J-aggregates.

3.8 AFM image of the chiral polymer-bound PIC J-aggregates

To get more direct evidence for the polymer-bound PIC J-aggregates after the addition of chiral $[Ru(phen)_3](PF_6)_2$, AFM was used to determine the microstructure. The image of the polymer-bound PIC J-aggregates was shown in Fig. 9. We can see that the chiral PAAS-PIC J-aggregates show

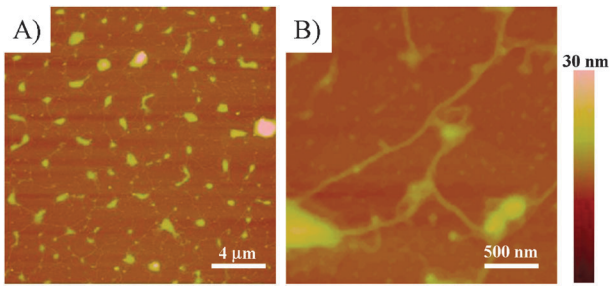

Fig. 9 AFM images of the polymer-bound PIC J-aggregates. (A) with low magnification; (B) with high magnification.

a nanowire-like morphology. However, no helical twisting morphology was observed for the individual nanowire. According to the reported literature, the handeness of the supermolecules may be oriented from intrinsic dissymmetry.[68]

Conclusions

In summary, the chiral supramolecular J-aggregates of Pseudoisocyanine could be formed in the presence of chiral multiple π-conjugated $[Ru(phen)_3](PF_6)_2$ in PAAS solution. The Cotton effect signal of the supermolecules depends on the absolute configuration of the $[Ru(phen)_3](PF_6)_2$ complex. This indicated the chiral induction was primarily based on the intramolecular π–π stacking. Most interestingly, the supramolecular chiral signal does not inversed when the excess chiral phenanthroline with the opposite configuration was added. It suggested the anionic polyelectrolyte induced chiral PIC supramolecular system has a chiral memory function. These findings may give us some insights on the mechanism of the chiral supramolecular self-assembly process by the non-covalent interaction.

Acknowledgements

This work was supported by the National Natural Science Foundation of China (Grant Nos. 20773098, 20877099 and 20972183) and the State Key Laboratory of Natural and Biomimetic Drugs (Grant No. 20080208), President Fund of GUCAS (A & B) and the 863 project of Ministry of Science and Technology of China (Grant No. 2008AA100801) and the Overall Strategic Cooperative Project between Guangdong Province and CAS (No. 2010B090300031).

References

1 J. J. D. de Jong, L. N. Lucas, R. M. Kellogg, J. H. van Esch and B. L. Feringa, *Science*, 2004, **304**, 278.
2 J. M. Lehn, *Science*, 2002, **295**, 2400.
3 L. Z. Zhao, X. Wang, Y. Li, R. J. Ma, Y. L. An and L. Q. Shi, *Macromolecules*, 2009, **42**, 6253.
4 S. Ghosh, X. Q. Li, V. Stepanenko and F. Wurthner, *Chem.–Eur. J.*, 2008, **14**, 11343.
5 M. Takeuchi, S. Tanaka and S. Shinkai, *Chem. Commun.*, 2005, 5539.
6 F. Allix, P. Curcio, N. P. Quoc, G. Pickaert and B. Jamart-Gregoire, *Langmuir*, 2010, **26**, 16818.
7 X. Huang, C. Li, S. G. Jiang, X. S. Wang, B. W. Zhang and M. H. Liu, *J. Am. Chem. Soc.*, 2004, **126**, 1322.
8 A. Ajayaghosh, R. Varghese, S. J. George and C. Vijayakumar, *Angew. Chem., Int. Ed.*, 2006, **45**, 1141.

Published on 22 August 2011 on http://pubs.rsc.org | doi:10.1039/C1CP20470J
Downloaded by Xiamen University on 07 April 2012

This journal is © the Owner Societies 2011

View Online

Downloaded by Xiamen University on 07 April 2012
Published on 22 August 2011 on http://pubs.rsc.org | doi:10.1039/C1CP20470J

9 H. Engelkamp, S. Middelbeek and R. J. M. Nolte, *Science*, 1999, **284**, 785.
10 K. Van den Bergh, I. Cosemans, T. Verbiest and G. Koeckelberghs, *Macromolecules*, 2010, **43**, 3794.
11 Y. W. Huang, Y. Yan, B. M. Smarsly, Z. X. Wei and C. F. J. Faul, *J. Mater. Chem.*, 2009, **19**, 2356.
12 J. Barbera, L. Puig, P. Romero, J. L. Serrano and T. Sierra, *J. Am. Chem. Soc.*, 2006, **128**, 4487.
13 S. Yagai, M. Gushiken, T. Karatsu, A. Kitamura and Y. Kikkawa, *Chem. Commun.*, 2011, **47**, 454.
14 M. Kimura, T. Hatanaka, H. Nomoto, J. Takizawa, T. Fukawa, Y. Tatewaki and H. Shirai, *Chem. Mater.*, 2010, **22**, 5732.
15 H. K. Murnen, A. M. Rosales, J. N. Jaworsk, R. A. Segalman and R. N. Zuckermann, *J. Am. Chem. Soc.*, 2010, **132**, 16112.
16 D. W. Bruce, P. Metrangolo, F. Meyer, T. Pilati, C. Prasang, G. Resnati, G. Terraneo, S. G. Wainwright and A. C. Whitwood, *Chem.–Eur. J.*, 2010, **16**, 9511.
17 M. M. L. Nieuwenhuizen, T. F. A. de Greef, R. L. J. van der Bruggen, J. M. J. Paulusse, W. P. J. Appel, M. M. J. Smulders, R. P. Sijbesma and E. W. Meijer, *Chem.–Eur. J.*, 2010, **16**, 1601.
18 L. W. Yan, Y. Xue, G. Gao, J. B. Lan, F. Yang, X. Y. Su and J. S. You, *Chem. Eur. J.*, 2010, **16**, 22507.
19 Y. Yang, M. Xue, J. F. Xiang and C. F. Chen, *J. Am. Chem. Soc.*, 2009, **131**, 12657.
20 M. Surin, P. G. A. Janssen, R. Lazzaroni, P. Leclere, E. W. Meijer and A. Schenning, *Adv. Mater.*, 2009, **21**, 1126.
21 I. Paraschiv, K. de Lange, M. Giesbers, B. van Lagen, F. C. Grozema, R. D. Abellon, L. D. A. Siebbeles, E. J. R. Sudholter, H. Zuilhof and A. T. M. Marcelis, *J. Mater. Chem.*, 2008, **18**, 5475.
22 L. X. Zeng, Y. J. He, Z. F. Dai, J. Wang, Q. Cao and Y. L. Zhang, *ChemPhysChem*, 2009, **10**, 954.
23 J. C. Xiao, J. L. Xu, S. Cui, H. B. Liu, S. Wang and Y. L. Li, *Org. Lett.*, 2008, **10**, 645.
24 C. F. J. Faul and M. Antonietti, *Adv. Mater.*, 2003, **15**, 673.
25 S. G. Chen, Y. C. Fu, G. T. Wang, G. Y. Li, Y. G. Ma, X. K. Jiang and Z. T. Li, *Tetrahedron*, 2010, **66**, 4057.
26 R. He, H. H. Song, Z. Wei, J. J. Zhang and Y. Z. Gao, *J. Solid State Chem.*, 2010, **183**, 2021.
27 A. J. Terpin, M. Ziegler, D. W. Johnson and K. N. Raymond, *Angew. Chem., Int. Ed.*, 2001, **40**, 157.
28 K. Biradha, C. Seward and M. J. Zaworotko, *Angew. Chem., Int. Ed.*, 1999, **38**, 492.
29 O. Mamula, A. von Zelewsky, T. Bark and G. Bernardinelli, *Angew. Chem., Int. Ed.*, 1999, **38**, 2945.
30 D. R. Xiao, E. B. Wang, H. Y. An, Y. G. Li, Z. M. Su and C. Y. Sun, *Chem.–Eur. J.*, 2006, **12**, 6528.
31 X. D. Chen, M. Du and T. C. W. Mak, *Chem. Commun.*, 2005, 4417.
32 Z. El-Hachemi, G. Mancini, J. M. Ribo and A. Sorrenti, *J. Am. Chem. Soc.*, 2008, **130**, 15176.
33 S. Malik, N. Fujita, M. Numata, K. Ogura and S. Shinkai, *J. Mater. Chem.*, 2010, **20**, 9022.
34 J. Cui, Y. Zheng, Z. Shen and X. Wan, *Langmuir*, 2010, **26**, 15508.
35 Y. F. Qiu, P. L. Chen and M. H. Liu, *Langmuir*, 2010, **26**, 15272.
36 M. M. Wang, G. L. Silva and B. A. Armitage, *J. Am. Chem. Soc.*, 2000, **122**, 9977.
37 Q. F. Yang, J. F. Xiang, Q. Li, W. P. Yan, Q. J. Zhou, Y. L. Tang and G. Z. Xu, *J. Phys. Chem. B*, 2008, **112**, 8783.
38 D. Mobius, *Adv. Mater.*, 1995, **7**, 437.
39 E. E. Jelley, *Nature*, 1936, **138**, 1009.
40 G. Scheibe, *Angew. Chem. Int. Ed.*, 1936, **49**, 563.
41 M. M. Demir, B. Ozen and S. Ozcelik, *J. Phys. Chem. B*, 2009, **113**, 11568.
42 Y. Kitahama, T. Yago, A. Furube and R. Katoh, *Chem. Phys. Lett.*, 2008, **457**, 427.
43 J. Knoester, *Phys. Lett. A*, 1993, **47**, 2083.
44 G. C. Zhang and M. H. Liu, *J. Mater. Chem.*, 2009, **19**, 1471.
45 G. T. Dempsey, M. Bates, W. E. Kowtoniuk, D. R. Liu, R. Y. Tsien and X. W. Zhuang, *J. Am. Chem. Soc.*, 2009, **131**, 18192.
46 B. Lohse, R. Vestberg, M. T. Ivanov, S. Hvilsted, R. H. Berg, C. J. Hawker and P. S. Ramanujam, *Chem. Mater.*, 2008, **20**, 6715.
47 W. J. Harrison, D. L. Mateer and G. J. T. Tiddy, *J. Phys. Chem.*, 1996, **100**, 2310.
48 T. Miyagawa, M. Yamamoto, R. Muraki, H. Onouchi and E. Yashima, *J. Am. Chem. Soc.*, 2007, **129**, 3676.
49 S. Kirstein, H. von Berlepsch, C. Bottcher, C. Burger, A. Ouart, G. Reck and S. Dahne, *ChemPhysChem*, 2000, **1**, 146.
50 Y. Z. Zhang, J. F. Xiang, Y. L. Tang, G. Z. Xu and W. P. Yan, *ChemPhysChem*, 2007, **8**, 224.
51 T. D. Slavnova, H. Gorner and A. K. Chibisov, *J. Phys. Chem. B*, 2007, **111**, 10023.
52 Q. F. Yang, J. F. Xiang, Q. Li, W. P. Yan, Q. J. Zhou, Y. L. Tang and G. Z. Xu, *J. Phys. Chem. B*, 2008, **112**, 8783.
53 O. K. Kim, J. Je, G. Jernigan, L. Buckley and D. Whitten, *J. Am. Chem. Soc.*, 2006, **128**, 510.
54 R. A. Garoff, E. A. Litzinger, R. E. Connor, I. Fishman and B. A. Armitage, *Langmuir*, 2002, **18**, 6330.
55 L. X. Zeng, Y. J. He, Z. F. Dai, J. Wang, C. Q. Wang and Y. G. Yang, *Sci. China, Ser. B: Chem.*, 2009, **52**, 1227.
56 J. A. Wang, D. D. Ding, L. X. Zeng, Q. A. Cao, Y. J. He and H. Zhang, *New J. Chem.*, 2010, **34**, 1394.
57 J. Wang, C. Y. Liu, D. D. Ding, L. X. Zeng, Q. Cao, H. Zhang, H. Zhao, X. J. Li, K. X. Xiang, Y. J. He and G. W. Wang, *New J. Chem.*, 2011, **35**, 1424.
58 K. Asakura, K. Kobayashi, Y. Mizusawa, T. Ozawa, S. Osanai and S. Yoshikawa, *Phys. D*, 1995, **84**, 72.
59 F. P. Dwyer, E. C. Gyarfas and D. P. Mellor, *J. Phys. Chem.*, 1955, **59**, 296.
60 K. A. McGee and K. R. Mann, *J. Am. Chem. Soc.*, 2009, **131**, 1896.
61 A. Werner, *Ber. Dtsch. Chem. Ges.*, 1912, **45**, 121.
62 A. Werner, *Ber. Dtsch. Chem. Ges.*, 1911, **44**, 1887.
63 R. Gaagel, R. Gadonas and A. Laubereau, *Chem. Phys. Lett.*, 1994, **217**, 228.
64 E. Daltrazzo, G. Scheibe, K. Gschwind and F. Haimerl, *Photogr. Sci. Eng.*, 1974, **18**, 441.
65 R. F. Pasternack, C. Fleming, S. Herring, P. J. Collings, J. dePaula, G. DeCastro and E. J. Gibbs, *Biophys. J.*, 2000, **79**, 550.
66 K. D. Belfield, M. V. Bondar, F. E. Hernandez, O. V. Przhonska and S. Yao, *Chem. Phys.*, 2006, **320**, 118.
67 C. Peyratout, E. Donath and L. Daehne, *J. Photochem. Photobiol., A*, 2001, **142**, 51.
68 O. Katzenelson and D. Avnir, *Chem.–Eur. J.*, 2000, **6**, 1346.